

# $\pi$ -Dimer from Bithiophene Radical Cations. Investigation of Equilibrium Constants as a Function of Substituent Size and Supporting Electrolyte Using Fast Conversion Electrochemical Cells

Andreas Neudeck,<sup>\*,a</sup> Pierre Audebert,<sup>b</sup> Laurent Guyard,<sup>b</sup> Lothar Dunsch,<sup>a</sup>  
Philippe Guiriec<sup>c</sup> and Philippe Hapiot<sup>\*,c</sup>

<sup>a</sup>IFW Dresden, Institut für Festkörperforschung, Abteilung Electrochemie und Leitfähige Polymere, Helmholtzstraße, 20, 01069 Dresden, Germany, <sup>b</sup>Laboratoire de Chimie Organique, Université de Franche Comté, La Bouloie, Route de Gray, 25030 Besançon, France and <sup>c</sup>Laboratoire d'Electrochimie Moléculaire de l'Université Denis Diderot (Paris 7), Unité de Recherche Associée au CNRS No. 438, 2 place Jussieu, Case Courrier No. 7107, 75251 Paris Cedex 05, France

**Dedicated to Professor Henning Lund on the occasion of his  
70th birthday.**

Neudeck, A., Audebert, P., Guyard, L., Dunsch, L., Guiriec, P. and Hapiot, P., 1999.  $\pi$ -Dimer from Bithiophene Radical Cations. Investigation of Equilibrium Constants as a Function of Substituent Size and Supporting Electrolyte Using Fast Conversion Electrochemical Cells. – Acta Chem. Scand. 53: 867–875. © Acta Chemica Scandinavica 1999.

The procedure for the determination of second order equilibrium constants  $K$ , using spectroelectrochemistry has been re-examined. Incomplete conversion of the starting material led to non-homogeneous concentration profiles and to considerable errors in the determinations of  $K$ . Values for three dialkylthiobithiophene radical cations have been measured in which the size of the thioalkyl group and of the counter anion of the supporting electrolyte are different. Large decreases observed in both cases may suggest that the association takes the form of a sandwich of two radical cations with the counter-anion in the middle.

In the last decade, well-defined oligomers have been extensively investigated as models for understanding the conducting properties of the corresponding polymers.<sup>1</sup> In this field, small oligothiophenes (as models of polythiophene) are by far the most studied systems.<sup>2,3</sup> Two likely conduction processes are envisaged: conduction along the thiophene ring chain via polarons/bipolarons<sup>4</sup> and conduction between different polymer chains passing through  $\pi$ -dimers and  $\pi$ -stacks. This last approach was based on recent spectroelectrochemical and ESR experiments performed with substituted terthiophenes. In this work, Miller and co-workers proposed that the radical cations of oligothiophenes exist in the form of either a monomer or a  $\pi$ -dimer depending on concentration and temperature conditions.<sup>5–8</sup> These intermolecular  $\pi$ -interactions may be strong in thin films and thus provide a mechanism for electrical conductivity. Similar experiments performed by other authors have confirmed these experimental observations with other oligothiophenes

using UV–VIS spectroscopy<sup>9–12</sup> or by cyclic voltammetry through the variation of the redox potentials. If the existence of the aggregate is well demonstrated and documented, less has been done to determine its chemical structure. For example, in an association composed of two positively charged species, the counter anion should play a fundamental role in both the  $\pi$ -dimer formation and the polymer conduction.<sup>13</sup> In crystal structure determinations of an end-capped terthiophene radical cation, it was found that the structure of this species involves  $\pi$ -stacks with close face-to-face contact of the molecules within the stack.<sup>14</sup> In addition to the possible  $\pi$ -dimerization, recent investigations concerning stabilized radical cations of oligothiophenes or oligopyrroles have demonstrated that reversible  $\sigma$ -dimerizations exist involving the reversible formation of intermolecular  $\sigma$ -bonds between the  $\pi$ -radical centres of the radical cations of polyene,<sup>15</sup> dimethylbithiophene<sup>16</sup> or small oligopyrroles.<sup>17</sup> Based on these observations, Smie and Heinze suggest that similar intermolecular  $\sigma$ -bonds between the  $\pi$ -radical centres are formed in the con-

\* To whom correspondence should be addressed.

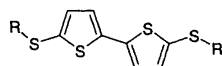
ducting polymer itself between different polymeric chains and that such reversible  $\sigma$ -dimerisations can account for several properties of conducting polymers. Thus if it is clear that reversible association exists between radical cations of oligomers, the structure of these 'dimers' in solution is still the subject of an active debate:  $\sigma$ -dimer,  $\pi$ -dimer, position and role of the counter-anion, etc.?

To gain new insight into the properties of these oligomers, we chose to investigate how the association equilibrium constants vary as function of the size of the substituents and of the nature of the supporting electrolyte. For such investigations, the radical cations need to be stabilized by substitution at the two terminal  $\alpha$ -positions to limit any irreversible chemical reactions (formation of higher oligomers, attack of a nucleophile, for example). For this reason, earlier studies were mainly related to chemically stabilized radical cations of oligomers.<sup>5-19</sup> In previous work, we have shown that the existence of the reversible association can easily be demonstrated (with determination of all the thermodynamic parameters) for the oxidation of oligothiophenes only by analysing the temperature and concentration dependences of the redox potentials in cyclic voltammetry experiments.<sup>18,19</sup> The advantage of this technique is that the timescale for observing the electrogenerated species is usually shorter during cyclic voltammetry experiments than for spectroelectrochemical experiments allowing the investigations of more unstable radical cations.<sup>20</sup> However, the errors made on the equilibrium constant determinations are generally larger than for the spectroelectrochemical measurements. In order to obtain better precision on  $K$  and to decrease the experimental measurement time, experiments were performed taking advantage of a recently developed spectroelectrochemical cell equipped with a gold honeycomb structure as an optical transparent electrode (gold-LIGA electrode).<sup>21-23</sup> Such a very thin cell permits total conversion of the substrate in around 1 s, allowing the observation of intermediates with half-lives between approximately 0.01 s and several minutes.<sup>21-23</sup>

In this paper, we present the preliminary results concerning the oxidation of three dialkylthiobithiophenes in the presence of different supporting electrolytes. In addition, we present a re-examination of the procedure to measure second-order equilibrium constants,  $K$ , in spectroelectrochemical cells. Indeed, the apparently straightforward spectroscopic procedure used in the previous literature investigations<sup>5-10</sup> if they demonstrate the existence of the dimer, can lead to considerable error on  $K$  due to the effects of gradient concentrations.

## Experimental

**Chemicals.** General procedure for 5,5'-dialkylthio-2,2'-bithiophene. 5,5'-Dialkylthio-2,2'-bithiophenes were pre-



Scheme 1.

pared by a modified procedure, which has been described for the synthesis of the 5,5'-dimethylthio-2,2'-bithiophene.<sup>5</sup> 2,2'-Bithiophene (1 g,  $6 \times 10^{-3}$  mol) was put into a dry flask under nitrogen with 10 ml of dry ether. The flask was cooled to 0 °C for 10 min and then BuLi (1.6 M in hexane, 7.6 ml, 12 mmol) was slowly added to the solution. After 1 h at 0 °C, dialkyl disulfide was added into the solution. The resulting solution was stirred at 0 °C for 10 min and then was allowed to warm to room temperature for 1 h. The mixture was then hydrolysed, the aqueous layer was extracted and both organic layers were washed and then dried over Na<sub>2</sub>SO<sub>4</sub>. The solvent was removed by rotary evaporation and the resulting mixture was purified by chromatography on silica gel with petroleum ether as the eluent. Yield 50–70%.

5,5'-Dimethylthio-2,2'-bithiophene: <sup>1</sup>H NMR (CDCl<sub>3</sub>):  $\delta$  2.50 (s, 6 H), 6.95 (s, 4 H). Analysis: Calc. C 46.47, H 3.90, S 49.62%. Found: C 46.32, H 3.80, S 49.88%.

5,5'-Diethylthio-2,2'-bithiophene: <sup>1</sup>H NMR (CDCl<sub>3</sub>):  $\delta$  1.30 (t, 6 H,  $J=7.3$  Hz), 2.85 (q, 4 H,  $J=7.3$  Hz), 6.98 (d, 2 H,  $J=3.7$  Hz), 7.01 (d, 2 H,  $J=3.7$  Hz). Analysis: Calc. C 50.30, H 4.92, S 44.77%. Found: C 50.41, H 4.86, S 44.73%.

5,5'-Dipropylthio-2,2'-bithiophene: <sup>1</sup>H NMR (CDCl<sub>3</sub>):  $\delta$  0.95 (t, 6 H,  $J=7.3$  Hz), 1.60 (sextet, 4 H,  $J=7.3$  Hz), 2.75 (t, 4 H,  $J=7.3$  Hz), 6.95 (d, 2 H,  $J=3.7$  Hz), 6.97 (d, 2 H,  $J=3.7$  Hz).

5,5'-Diisopropylthio-2,2'-bithiophene: <sup>1</sup>H NMR (CDCl<sub>3</sub>):  $\delta$  1.30 (d, 12 H,  $J=6.7$  Hz), 3.15 (m, 2 H,  $J=6.7$  Hz), 7.02 (s, 4 H). Analysis: Calc. C 53.45, H 5.76, S 40.77%. Found: C 53.24, H 5.73, S 41.03%. All other chemicals were commercially available and were purchased from Aldrich. Supporting electrolytes were recrystallized from water–ethanol mixtures and dried over P<sub>2</sub>O<sub>5</sub> under a nitrogen atmosphere.

**Electrochemical apparatus.** Cyclic voltammetry: all the cyclic voltammetry experiments were carried out at  $20 \pm 0.1$  °C with a three-electrode set-up using a cell equipped with a jacket allowing circulation of water from the thermostat. The counter-electrode was a Pt wire and the reference electrode an aqueous saturated calomel electrode ( $E^\circ/\text{SCE} = E^\circ/\text{NHE} - 0.2412$  V) with a salt bridge containing the supporting electrolyte. The SCE electrode was checked against the ferrocene/ferricinium couple ( $E^\circ = +0.405$  V/SCE) before and after each experiment. The working electrode was a 1 mm diameter gold or platinum disk. The electrode was carefully polished before each set of voltammograms with 1 mm diamond paste and ultrasonically rinsed in absolute ethanol. Electrochemical instrumentation consisted of a PAR Model 175 Universal programmer and a home-built potentiostat equipped with a positive feedback compensation device.<sup>24</sup> The data were acquired with a 310 Nicolet oscilloscope.

Spectroelectrochemical experiments were performed with a capillary slit-cell for UV–VIS spectroscopy using

gold-LIGA-structures as an optical transparent electrode.<sup>21–23</sup> The gold-LIGA-foil used had a thickness of 100  $\mu\text{m}$  and a honeycomb structure with hexagon holes of 20  $\mu\text{m}$  diameter and the thickness of the walls between the holes was 15  $\mu\text{m}$ . The gold-LIGA structure was fixed in a capillary slit of 150  $\mu\text{m}$ . Complete electrochemical conversion in the capillary slit occurred in less than 2 s. A silver wire coated with silver chloride was used as pseudo-reference electrode in the spectroelectrochemical cell. The whole cell was electrically isolated and immersed in a cooling bath. The spectra were recorded with a fast scanning (3 ms per spectra) diode array spectrophotometer (J. and M. Analytische Mess-und Regeltechnik GmbH, Aalen, Germany). A 75 W xenon lamp and the spectrophotometer were connected by optical wave guides with the LIGA cell. During one complete experiment (forward and reverse scan), spectra are recorded with a fixed interval time between each spectra. The interval time was adjusted as function of the scan rate (0.01–0.1  $\text{V s}^{-1}$ ) for recording 60 spectra during one experiment. In order to minimise any photochemical degradation of the oligomer during the course of the spectroelectrochemical experiments, the light intensity was decreased by placing the optical wave-guides at an appropriate distance from the entrance of the cell and keeping the shutter of the lamp closed between the recording of successive spectra.

## Results and discussion

*Electrochemical behaviour of dialkylthiobithiophenes.* The cyclic voltammograms of 2,2'-dialkylthiobithiophenes are similar to the first one of the series [5,5'-(methylthio)-bithiophene] which has previously been described in detail.<sup>5</sup> They show two mono-electronic oxidation waves in the potential range 0.9–1.1 V vs. SCE. The two waves have close oxidation potentials but the difference is large enough to allow the characterisation of the first cyclic voltammetric wave as a reversible wave at the lowest scan rates (less than 10  $\text{mV s}^{-1}$ ). The second wave becomes reversible only at higher scan rates indicating that the oxidation product of the second wave is less stable with a lifetime of less than 1 s. From this observa-

**Table 1.** Formal oxidation potentials from cyclic voltammetry in acetonitrile at 20 °C

Substituent	$E^{\circ}_{\text{ox1}}/\text{V (SCE)}^a$	$E^{\circ}_{\text{ox2}}/\text{V (SCE)}^a$
SCH <sub>3</sub>	0.895	1.083
SC <sub>2</sub> H <sub>5</sub>	0.924	1.092
SCH(CH <sub>3</sub> ) <sub>2</sub>	0.987	1.082

<sup>a</sup>Measured as the half-sum of the anodic and cathodic peak potentials. Error  $\pm 5$  mV.

tion, it is immediately deduced that the first wave corresponds to the formation of the radical cation and the second to its further oxidation to the dication.

This is supported by UV–VIS spectroelectrochemical measurements. At the potential of the first wave, the band of the starting material in the range of 300–350 nm disappeared and two strong absorption bands in the range 540–560 and 840–900 nm, as well as three weaker bands in the ranges 440–460, 650–670, and 830–870 nm appeared simultaneously. When the potential of the second cyclic voltammetric wave was reached, these bands disappeared and a new strong band at around 500 nm was observed. However, relatively fast dication decay made it difficult to obtain the spectrum of the dication itself during a slow cyclic voltammetric scan under our experimental conditions and the absorbances of the follow-up products were mainly detected. Measurements at lower temperatures clearly showed that it is not only the formation of the radical cation that influences the first electron transfer, in agreement with literature results.<sup>5–7</sup> As previously described for similar oligothiophenes<sup>5–7,10,15,16</sup> when the temperature was lowered, the intensities of both strong absorption bands decreased and the other three bands showed a net increase. This observation shows that these bands correspond to different species and that their ratio is temperature-sensitive. This has been explained by a reversible dimerisation of the radical cation leading to a  $\pi$ -dimer<sup>5–7</sup> or  $\sigma$ -dimer.<sup>15,16</sup>

*Determination of the second-order equilibrium constant in spectroelectrochemical cells.* The reversible dimerisation

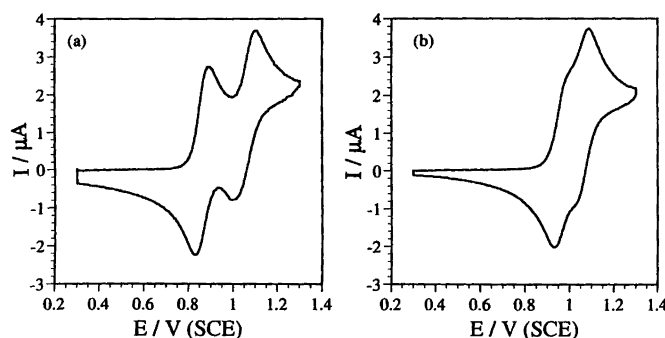
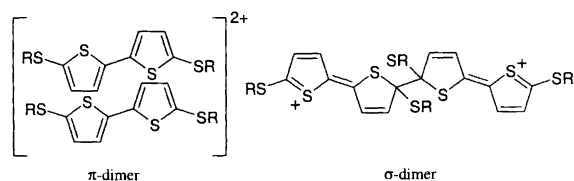
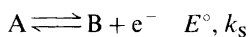


**Fig. 1.** Cyclic voltammetry on a 1 mm diameter gold disk electrode of dialkylthiobithiophene ( $c^{\circ} = 1.7 \times 10^{-3} \text{ mol l}^{-1}$ ) in ACN + 0.1  $\text{mol l}^{-1}$  of  $\text{NBu}_4\text{PF}_6$ .  $T = 20$  °C. Scan rate = 0.2  $\text{V s}^{-1}$ . (a)  $\text{CH}_3\text{S-2T-SCH}_3$ ; (b)  $(\text{CH}_3)_2\text{HCS-2T-SCH}(\text{CH}_3)_2$ .



Scheme 2. Schematic structures of proposed  $\pi$ -dimer and  $\sigma$ -dimer.

mechanism can be written as:



where A is the dialkylthiobithiophene, B its cation-radical and D the corresponding dimer. In this case, the ratio of the radical cation to the dimer depends on the concentration and the temperature. From cyclic voltammetry experiments performed with related oligothiophenes, we have found that this equilibrium is fast<sup>18,19</sup> and thus that the concentrations ratio is simply given by  $K = c_D/c_B^2$ . Replacing the concentrations by absorbances using the Beer–Lambert law leads to  $c_i = A_i/\epsilon_i d = A_i/\tilde{\epsilon}_i$  ( $\epsilon$ , absorptivity coefficient;  $d$ , optical pathway). By use of this simple law, a plot of the logarithm of the absorbance of the dimer versus that of the radical cation leads to the determination of  $K$  and of the ratio of the  $\epsilon$ :

$$\ln(A_D) = 2 \ln(A_B) + \ln(K_{\text{dim}}) + \ln\left(\frac{\tilde{\epsilon}_D}{\tilde{\epsilon}_B^2}\right).$$

It shows that a slope of two is expected in the case of a dimerisation process between two radical cations. This test has already been applied with success when the radical cation was produced by a photochemical process to prove the second-order nature of the equilibrium expected for dimerisation between two radical cations.<sup>6</sup> It is notable that, in such a situation, the concentration profiles are almost constant in the cell if the absorbance of the starting oligomer is not too high at the excitation wavelength. The values of  $K$  (and the ratio between the two  $\epsilon$ ) can also be obtained from the origin intercept from a series of spectra recorded at different concentrations of radical cations. An extension of this treatment, which was used in previous investigations, is to consider a series of spectra recorded during electrolysis when the radical cation is generated at an electrode. We applied such treatment to our data recorded in the LIGA cell. We plotted the variation of the logarithm of the absorbance of the dimer versus the logarithm of the absorbance of the radical cation formed during the cyclic voltammogram. In principle, this is very similar to the procedure in which these data are plotted at different times during electrolysis.<sup>5–7</sup> The experimental data for the oxidation of  $C_2H_5S-2T-SC_2H_5$  (see Fig. 2) do not show a linear dependence and the apparent slopes are much lower than the expected value of 2. A hook-shaped curve was observed in the temperature range  $-40$  to  $60^\circ\text{C}$ . It is therefore evident that the different possible mechanisms cannot be straightforwardly distinguished.

Table 2. Spectral characteristics of the bithiophenes ( $\lambda_{\text{max}}/\text{nm}$ ) in acetonitrile.

	Neutral	Radical cation	Dimer
SCH <sub>3</sub>	346	490, 560, 880	450, 670, 880
SC <sub>2</sub> H <sub>5</sub>	340	490, 562, 885	452, 675, 890
SCH(CH <sub>3</sub> ) <sub>2</sub>	340	498, 565, 890	457, 685, 890

This arises because in dimerisation equilibrium constant determinations, the concentrations in the solution have been considered as constant throughout the cell.<sup>5–10</sup> This situation is only achieved after complete conversion of all the starting oligomers assuming that the radical cation produced is chemically stable for the duration of the experiment. Such conditions are rarely obtained in classical thin cells of several millimetre lengths, and certainly not during the electrolysis at constant potential when the radical cation is being produced. Therefore, to estimate the influence of the concentration gradient inside the spectroelectrochemical cell over the time period or during the cyclic voltammogram scan, explicit difference-finite simulations<sup>25</sup> based on the reversible dimerisation mechanism<sup>26</sup> were applied for finite diffusion conditions and for different cell-lengths. The amounts of substance for each species, which are proportional to the absorbance signal detected from the spectroelectrochemical measurements, were calculated from the integrals of the concentration over the optical pathway:

$$n_i = \int_0^{x_{\text{slit}}} c_i(x) dx$$

A double logarithmic plot of  $n_{\text{dimer}}$  (amount of generated dimer) versus  $n_{\text{radical cation}}$  (amount of generated radical cation) for a fast electron transfer (Nernstian behaviour) and fast chemical equilibrium shows exactly the hook-shaped behaviour as observed from the experimental data (see Figs. 3 and 4). The slope varies from 2, in the range where the generated amount is too small to be detected under experimental conditions, to 1.25 in the range used for the experimental data.

The simulation of the *in-situ* spectroelectrochemical data clearly shows that the non-linear behaviour of the plot of absorbance of the dimer versus that of the radical cation arises from the concentration gradient on the optically transparent electrode. Therefore, it is necessary to use only the spectra recorded after a complete conversion of the oligomer into the radical cation in the capillary slit to characterise the mechanism and evaluate the thermodynamic parameters. The spectroelectrochemical cell based on LIGA structures permit rapid conversion inside the hexagon tubes of honeycombed microstructure in a diffusion-limited range in less than 1 s after the potential step with capillary diameters of ca.  $20 \mu\text{m}$ .<sup>21–23</sup> For our dialkylthiobithiophenes, the small separation between the first and second oxidation waves makes it difficult to use potential step experiments to form only the species generated at the level of the first

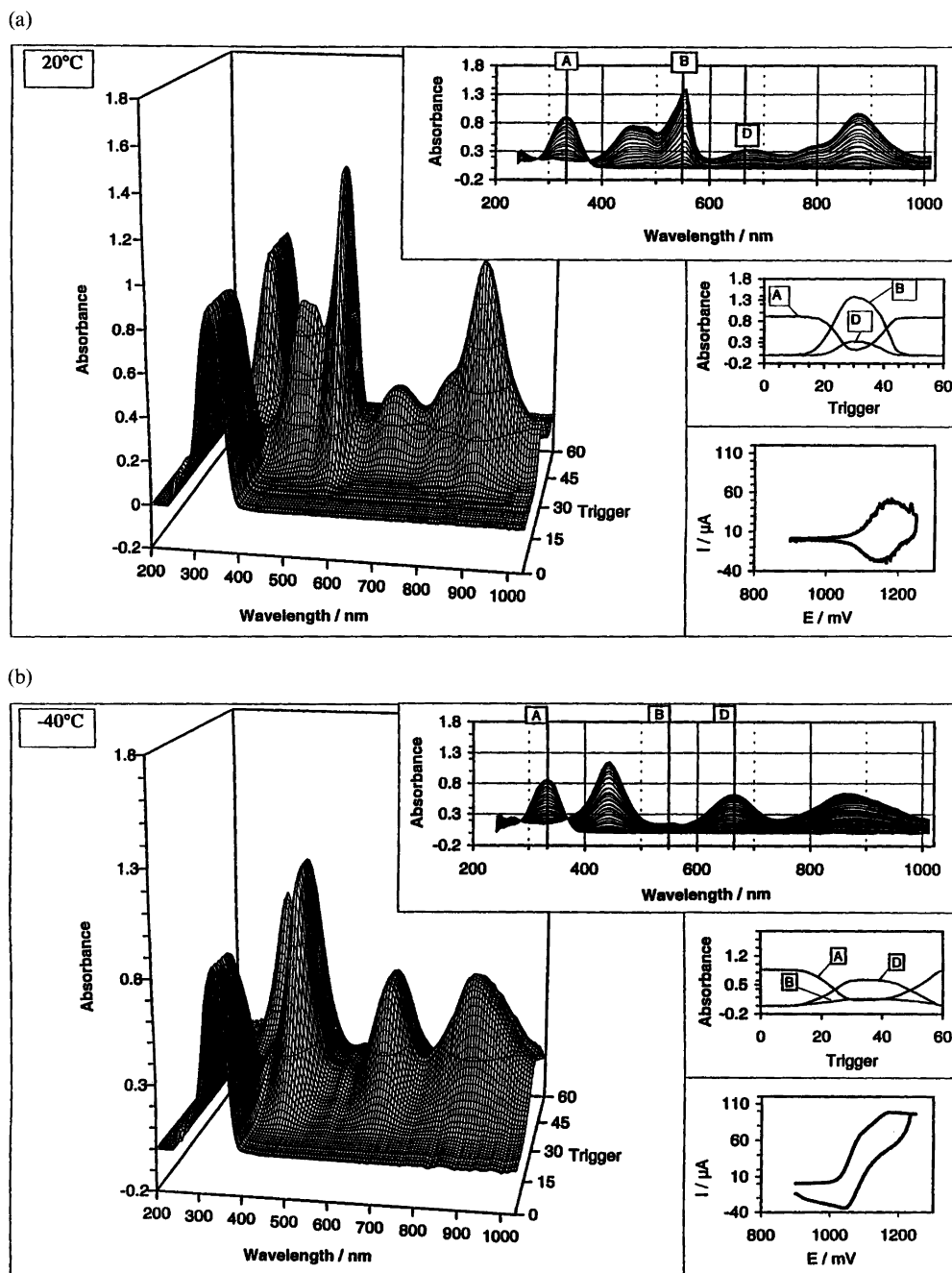


Fig. 2. Spectroelectrochemistry of a solution of  $C_2H_5S-2T-SC_2H_5$  ( $c^\circ = 3.5 \text{ mol l}^{-1}$ ) in  $ACN + 0.1 \text{ mol l}^{-1}$  of  $NBu_4PF_6$ . 3D-plot, cyclic voltammogram and absorbances variations corresponding to the neutral oligomer (A), radical-cation (B) and dimer (D) during the same cyclic voltammetric experiment at 20 and  $-40^\circ\text{C}$  for the oxidation of  $C_2H_5S-2T-SC_2H_5$ . Scan rate =  $20 \text{ mV s}^{-1}$ . The potential scale is referred to the  $Ag/Ag^+$  pseudo-reference electrode.

oxidation process, which are easier to control during cyclic voltammetry experiments. The use of the cyclic voltammetric potential regime also has an additional advantage. With the two equilibrated spectra, the spectrocyclic voltammograms may also contain the spectra of the decomposition products coming from the second oxidation. At slow scan rates in the range  $5\text{--}50 \text{ mV s}^{-1}$ , the dication is chemically unstable and only the spectrum of the follow-up product is visible (the spectrum of the dication was not observable).

The dimerisation of the radical cation is accompanied by an increase of the state of order of the system, therefore the standard reaction entropy  $\Delta_R S^\circ$  is negative and the dimer is expected to be favoured at the lowest temperatures. This permits the assignment of the spectra in the forward scan at  $20^\circ\text{C}$ , which contain mainly the absorbances of the radical cation superimposed by the spectra of a small amount of the dimer (and possibly of follow-up products coming from the dication decay). The same spectra at  $-40^\circ\text{C}$  correspond only to the

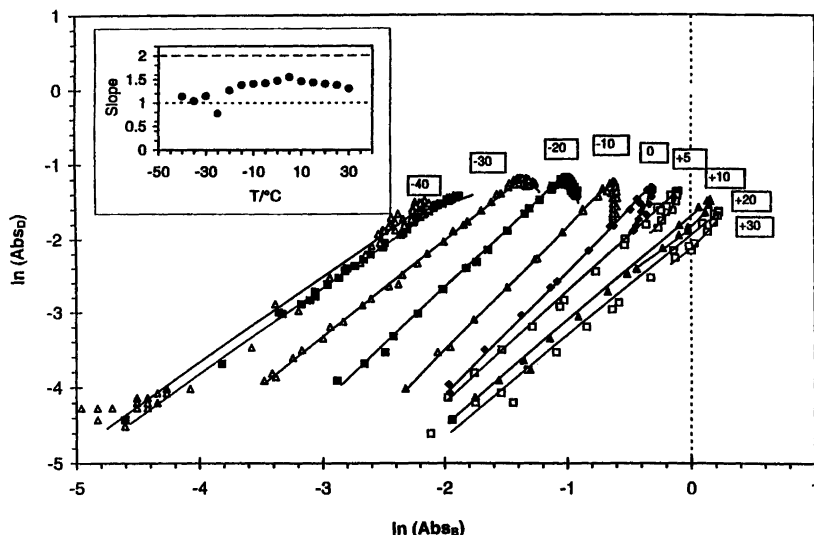


Fig. 3. Plot of the absorbance of the dimer (D) ( $\lambda=670$  nm) versus the absorbance of the radical cation (B) ( $\lambda=560$  nm) during cyclic voltammetry at different temperatures for the oxidation of  $\text{CH}_3\text{S-2T-SCH}_3$  ( $c^\circ=2 \times 10^{-3} \text{ mol l}^{-1}$ ) in  $\text{ACN} + 0.1 \text{ mol l}^{-1} \text{ NBu}_4\text{PF}_6$  in gold LIGA-Cell. Scan rate =  $20 \text{ mV s}^{-1}$ .

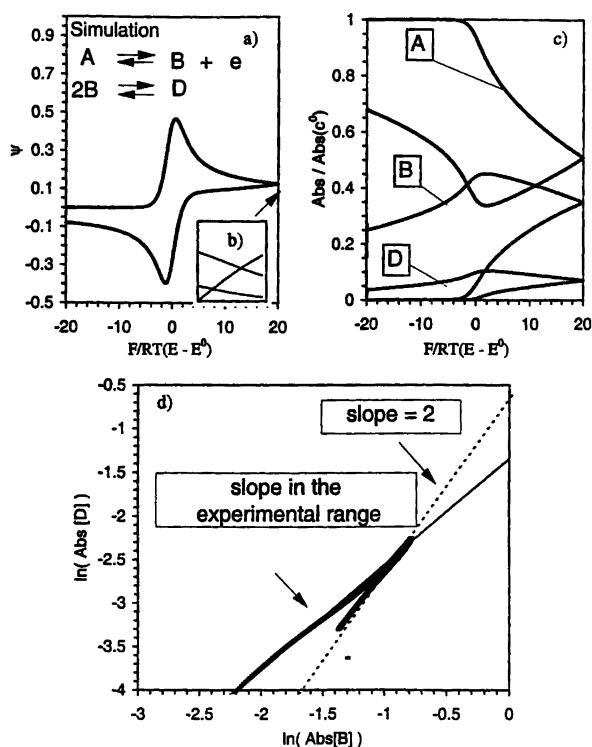


Fig. 4. Simulation of the observed double logarithmic plot of the absorbance of the dimer versus the radical cation under finite conditions during a cyclic voltammetry experiment ( $D=1.5 \times 10^{-5} \text{ cm}^2 \text{ s}^{-1}$ ,  $\nu=100 \text{ mV s}^{-1}$ ,  $c^\circ=10^{-3} \text{ mol l}^{-1}$ ,  $K=2000 \text{ l mol}^{-1}$  and a slit of width  $200 \mu\text{m}$ ). (a), (b) Voltammogram and profile concentrations at the level of the switching potential.  $\psi$  = normalized current =  $i/i_{\text{diffusion}}$ . (c) Variation of the normalised absorbances with the applied potential during the scan. (d) log-log plot. The continuous line (—) is the apparent variation obtained from a linear fit compared with the expected slope of 2 (---).

dimer superimposed by a very minor amount of the radical cation and only traces of the product of the second wave. Using the spectrum of the products of the second wave (obtained at the switching potential) and of the starting material (at the initial potential), the separated spectrum of the starting material, radical cation, dimer and of the final products can be obtained using an iterative procedure via factor analysis, which has been described in detail in Refs. 22 and 23. The four separated spectra can be used to obtain the individual absorbances of each species  $i$  [ $A_i(T)$ ] at any chosen wavelength and temperature  $T$ , and for each potential. As observed in Fig. 3, during the potential scan, the amounts of radical cation (or of the dimer at low temperature) first increase when the applied potential approaches the level of the first oxidation wave and then start to decrease when the direction of the scan is reversed or if the applied potential becomes close to the second oxidation process. Therefore, the scan rate has to be low enough to allow almost complete oxidation of the bithiophene before the level of the second wave is reached. We found that a scan rate of  $20 \text{ mV s}^{-1}$  allows these conditions to be fulfilled. Thus in the following treatments, the absorbances of the dimer and of the radical cation  $A_D(T)$  and  $A_B(T)$  were taken from the spectra showing the maximum absorbance of the dimer. Using these values, the values of  $\epsilon_D d$  and of  $\epsilon_B d$  can be obtained by the following linear regression (see the Appendix) and then allow the measurement of  $K$  at each temperature:

$$\frac{\left( \frac{A_{A,\text{init}}(T) - A_A(T)}{A_{A,\text{init},T_{\text{max}}}} - \frac{A_P(T)}{A_{P,\text{sw}}} \right) C_{\text{init}}}{A_B(T)} = \frac{1}{\epsilon_B d} + \frac{2}{\epsilon_D d} \left( \frac{A_D(T)}{A_B(T)} \right)$$

where  $C_{\text{init}}$  is the concentration of dialkylthiobithiophene in the solution,  $A_{A,\text{init}}(T)$ ,  $A_{A,\text{init}}(T_{\text{max}})$  are the initial

absorbances of the starting dialkylthiobithiophenes measured before the oxidation at the beginning of the scan at temperature  $T$  and at the highest used temperature,  $A_p(T)$ ,  $A_{p,sw}(T)$  are the absorbances of the products formed at the level of the second oxidation at the current and switching potentials,  $A_D(T)$ ,  $\epsilon_D$ ,  $A_B(T)$ ,  $\epsilon_B$  are the absorbances and absorptivity coefficients of the dimer and radical cation and  $d$  is the optical length.

The thermodynamic parameters  $\Delta_R H^\circ$ ,  $\Delta_R S^\circ$  and the ratio of the absorptivity coefficients can be directly determined by a more elegant treatment using a non-linear fit where only the individual absorbances  $A_i(T)$  need to be known (see the Appendix):

$$\ln \left\{ \left( \frac{A_{\text{ratio}}(T)}{\epsilon_{\text{ratio}}} \right)^2 + \frac{A_{\text{ratio}}(T)}{\epsilon_{\text{ratio}}} \right\} - \ln [c_{\text{gen}}(T)] \\ = -\frac{\Delta_R H^\circ}{RT} + \frac{\Delta_R S^\circ}{R}$$

with

$$A_{\text{ratio}}(T) = \frac{A_D(T)}{A_B(T)}, \quad \epsilon_{\text{ratio}} = \frac{\epsilon_D}{\epsilon_B}$$

and

$$c_{\text{gen}}(T) = c_{\text{init}} \left( \frac{A_{A,\text{init}}(T) - A_A(T)}{A_{A,i}(T_{\text{max}})} - \frac{A_p(T)}{A_{p,sw}} \right)$$

Both treatments give similar results. An example of this treatment is presented in Fig. 5 for the oxidation of the MeS-2T-SMe.  $c_{\text{init}}$  is the concentration of dialkylthiobithiophene in the solution and  $c_{\text{gen}}(T)$  the real concentration of radical cation produced (in the dimer form or free radical cation form). In many experiments (see for example the relative variation  $c_{\text{gen}}/c_{\text{init}}$  in Fig. 5), we noticed a decrease of  $c_{\text{gen}}$  with the temperature even when complete oxidation of the bithiophene was achieved. This effect was less visible at lower concentration ( $c_{\text{init}} < 10^{-3} \text{ mol l}^{-1}$ ) and seems due to the diminution of the oligomer solubility at low temperature and explains the necessity of a concentration correction in the data treatment. An example of this procedure is illustrated in Fig. 5 with the variation of the corrected absorbance  $A_i(T)/\text{corr}$  where corr is the relative variation of the total amount of radical cation (in the dimer form or free radical cation form)  $c_{\text{gen}}/c_{\text{init}}$ . When the temperature decreases, the absorbance of the radical cation decreases as the absorbance of the dimer increases. The derived free enthalpy shows a good linear dependence with the temperature justifying the data treatment. From repetitive experiments, we found that the error on the measurements of the individual  $\Delta_R H$  and  $\Delta_R S$  were around 10%. The error on the corresponding dimerisation equilibrium constants at 25 °C,  $K_{298}$ , were estimated to be around 20%.

In this preliminary study, thermodynamic constants were determined for three dialkylthiobithiophenes in which the size of the substituents was changed (Table 3). It is clear that the equilibrium constants are sensitive to

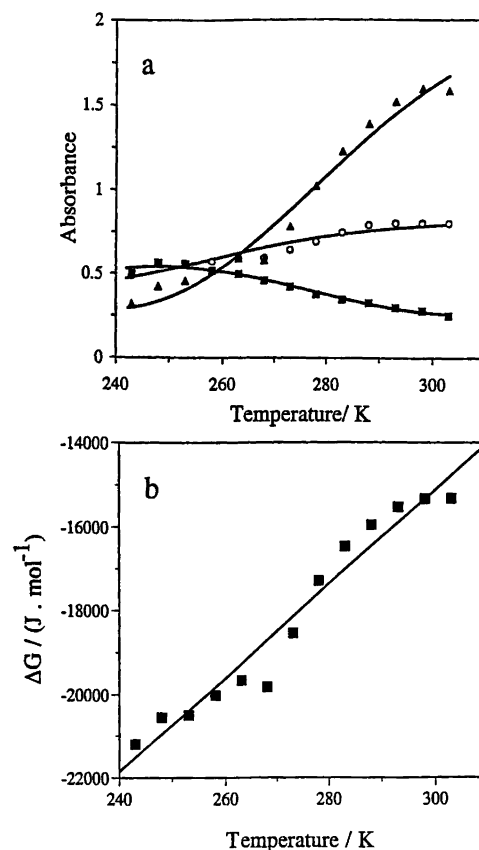


Fig. 5. Oxidation of  $\text{CH}_3\text{S-2T-SCH}_3$  ( $c^\circ = 2 \times 10^{-3} \text{ mol l}^{-1}$ ) in acetonitrile +  $0.1 \text{ mol l}^{-1} \text{ NBu}_4\text{PF}_6$ . (a) Variation of the corrected absorbance with the temperature for the dimer ( $\lambda = 560 \text{ nm}$ ) (■) and the radical-cation ( $\lambda = 670 \text{ nm}$ ) (▲). The relative variation of the total amount of radical-cation produced in the dimer form or free radical-cation form  $c_{\text{gen}}/c_{\text{init}}$  is also represented (○). (b) Variation of the corresponding free enthalpy with the temperature.

the size of the alkylthio substituent. A decrease by a factor of ten is observed on going from methylthio to the isopropylthio. Similarly, we have also investigated the counter-anion effects on the stability of the dimer. Use of three types of anion, which are known to be well-dissociated in organic solvents, allowed us to test the effects of the anion size on the stability of the dimer. Small decreases were observed between  $\text{PF}_6^-$  and  $\text{ClO}_4^-$  whereas, in contrast, a large decrease was found when using  $\text{N}(\text{SO}_2\text{CF}_3)^-$ . Although other determinations are required to confirm this tendency, the large variation observed with the anions appears consistent with an association between two radical cations with the counter-anion located between them, as proposed previously on the bases of theoretical calculations.<sup>13</sup>

## Conclusions

The procedure for the determination of second-order equilibrium constant using spectroelectrochemistry has been re-examined. In such experiments, great care should be taken to reduce the conversion time of the cell not

Table 3. Thermodynamic data of the dimer formation.<sup>a</sup>

Substituent	Electrolyte								
	Et <sub>4</sub> NClO <sub>4</sub>			NBu <sub>4</sub> PF <sub>6</sub>			LiN(SO <sub>2</sub> CF <sub>3</sub> ) <sub>2</sub>		
	$\Delta_R H^\circ /$ kJ mol <sup>-1</sup>	$\Delta_R S^\circ /$ J mol <sup>-1</sup> K <sup>-1</sup>	$K_{298}$	$\Delta_R H^\circ /$ kJ mol <sup>-1</sup>	$\Delta_R S^\circ /$ J mol <sup>-1</sup> K <sup>-1</sup>	$K_{298}$	$\Delta_R H^\circ /$ kJ mol <sup>-1</sup>	$\Delta_R S^\circ /$ J mol <sup>-1</sup> K <sup>-1</sup>	$K_{298}$
SCH <sub>3</sub>	-51	-110	1400	-49	-110	530	-46	-115	110
SC <sub>2</sub> H <sub>5</sub>				-47	-110	350			
SCH(CH <sub>3</sub> ) <sub>2</sub>	-51	-130	120	-42	-100	170			

<sup>a</sup>Errors on  $\Delta_R H^\circ = \pm 5$  kJ mol<sup>-1</sup>,  $\Delta_R S^\circ = \pm 10$  J mol<sup>-1</sup> K<sup>-1</sup> and  $K_{298} \pm 20\%$ .

only to avoid the chemical decomposition of the radical cation, but also because incomplete conversion conditions lead to non-homogeneous concentration profiles and thus to considerable errors in the determinations of  $K$ . Better determinations also required the separation of the spectra into their individual components to obtain the real absorbance of the radical cation and of its dimer. In a preliminary study, we have used this approach to determine the  $K$  values for three dialkylthiobithiophene radical cations in which both the size of the alkyl group and of the counter-anion of the supporting electrolyte were changed. Large decreases were observed in both cases which may suggest that an association takes place in which two radical cations sandwich the anion in the middle. Work is presently in progress to confirm this hypothesis with other types of substituent and anion as previously proposed.

## Appendix

For a dimerization equilibrium assuming that the concentration are almost homogeneous, the value of  $K$  can be evaluated from the classical expression:

$$K_{\text{dim}} \approx \frac{n_{\text{D,generated}}(E_{\text{D,max}})/V_{\text{slit}}}{[n_{\text{B,generated}}(E_{\text{D,max}})/V_{\text{slit}}]^2} = \frac{A_{\text{D}}(\lambda_{\text{D}}, E_{\text{D,max}})}{\tilde{\varepsilon}_{\text{D}}(\lambda_{\text{D}})} \left( \frac{A_{\text{B}}(\lambda_{\text{B}}, E_{\text{D,max}})}{\tilde{\varepsilon}_{\text{B}}(\lambda_{\text{B}})} \right)^2$$

$$= \left( \frac{A_{\text{D}}(\lambda_{\text{D}}, E_{\text{D,max}})}{A_{\text{B}}(\lambda_{\text{B}}, E_{\text{D,max}})} \right) \left( \frac{\tilde{\varepsilon}_{\text{B}}(\lambda_{\text{B}})^2}{\tilde{\varepsilon}_{\text{D}}(\lambda_{\text{D}})} \right) \quad (1)$$

Therefore, the equilibrium constant of the dimerization can be calculated at a selected temperature from the  $A_i(\lambda_i, E_{\text{D,max}})$  values for the radical cation and the dimer obtained after separation of the superimposed spectra at the potential where the dimer shows a maximum if the absorbance coefficients  $\tilde{\varepsilon}_i(\lambda_i)$  of the dimer and the radical cation are known. The total quantity of radical cation  $n_{\text{gen}}$  present in the solution in free or associated forms  $n_{\text{B}}, n_{\text{D}}$  is equal to the initial amount of bithiophene  $n_{\text{init}}$  minus the residual quantity of bithiophene minus the amount of product lost because of interference from the second oxidation wave, eqn. (2).

$$n_{\text{gen}}(T) = n_{\text{B}}(T) + 2n_{\text{D}}(T) = n_{\text{init}} - n_{\text{A}}(T) - n_{\text{P}}(T) \quad (2)$$

Considering a homogeneous distribution of all species at the initial and switching potential as well as at the potential where the amount of dimer shows a maximum during the forward potential scan, the amounts of substances can be replaced by their concentrations  $c_i = n_i/V_{\text{slit}}$  and then by their absorbances, eqn. (3):

$$\frac{A_{\text{A}}(\lambda_{\text{A}}, E_{\text{init}}, T)}{\varepsilon_{\text{A}}(\lambda_{\text{A}})} - \frac{A_{\text{A}}(\lambda_{\text{A}}, E_{\text{D,max}}, T)}{\varepsilon_{\text{A}}(\lambda_{\text{A}})} - \frac{A_{\text{P}}(\lambda_{\text{P}}, E_{\text{D,max}}, T)}{\varepsilon_{\text{P}}(\lambda_{\text{P}})}$$

$$= \frac{A_{\text{B}}(\lambda_{\text{B}}, E_{\text{D,max}}, T)}{\varepsilon_{\text{B}}(\lambda_{\text{BA}})} + 2 \frac{A_{\text{D}}(\lambda_{\text{D}}, E_{\text{D,max}}, T)}{\varepsilon_{\text{D}}(\lambda_{\text{DA}})} \quad (3)$$

The absorptivity coefficients can be obtained from eqns. (4) and (5).

$$\varepsilon_{\text{A}}(\lambda_{\text{A}})d = \frac{A_{\text{A}}(\lambda_{\text{A}}, E_{\text{init}}, T_{\text{max}})}{c_{\text{init}}} \quad \text{and} \quad (4)$$

$$\varepsilon_{\text{P}}(\lambda_{\text{P}})d = \frac{A_{\text{P}}(\lambda_{\text{P}}, E_{\text{init}}, T_{\text{max}})}{c_{\text{init}}}$$

$$\left( \frac{A_{\text{A}}(\lambda_{\text{A}}, E_{\text{init}}, T) - A_{\text{A}}(\lambda_{\text{A}}, E_{\text{D,max}}, T)}{A_{\text{A}}(\lambda_{\text{A}}, E_{\text{in}}, T_{\text{max}})} - \frac{A_{\text{P}}(\lambda_{\text{P}}, E_{\text{D,max}}, T)}{A_{\text{P}}(\lambda_{\text{P}}, E_{\text{sw}}, T_{\text{max}})} \right) c_{\text{init}}$$

$$= \frac{A_{\text{B}}(\lambda_{\text{B}}, E_{\text{D,max}}, T)}{\varepsilon_{\text{B}}(\lambda_{\text{B}})d} + 2 \frac{A_{\text{D}}(\lambda_{\text{D}}, E_{\text{D,max}}, T)}{\varepsilon_{\text{D}}(\lambda_{\text{D}})d} \quad (5)$$

There are only two unknown parameters unknown in eqn. (5): the absorbance coefficients of the radical cation and dimer. Equation (5) can be linearized as eqn. (6).

$$\left( \frac{A_{\text{A}}(\lambda_{\text{A}}, E_{\text{in}}, T) - A_{\text{A}}(\lambda_{\text{A}}, E_{\text{D,max}}, T)}{A_{\text{A}}(\lambda_{\text{A}}, E_{\text{init}}, T_{\text{max}})} - \frac{A_{\text{P}}(\lambda_{\text{P}}, E_{\text{D,max}}, T)}{A_{\text{P}}(\lambda_{\text{P}}, E_{\text{sw}}, T_{\text{max}})} \right) c_{\text{init}}$$

$$= \frac{1}{\varepsilon_{\text{B}}(\lambda_{\text{B}})d} + \frac{2}{\varepsilon_{\text{D}}(\lambda_{\text{D}})d} \left( \frac{A_{\text{D}}(\lambda_{\text{D}}, E_{\text{D,max}}, T)}{A_{\text{B}}(\lambda_{\text{B}}, E_{\text{D,max}}, T)} \right) \quad (6)$$

In other words, a plot of temperature dependence of the real amount of radical cation and dimer divided by the absorbance of the radical cation versus the quotient of the absorbance of the dimer and the radical cation yields shows a linear dependence with a slope of  $2/\varepsilon_{\text{D}}d$  and an intercept of  $1/\varepsilon_{\text{B}}d$ .

The standard reaction enthalpy  $\Delta_R H^\circ$  and entropy



$\Delta_R S^\circ$  can also be evaluated by a more elegant procedure in which only the ratio of the absorbance of the dimer to the radical cation need to be known. The product of the eqns. (1) and (2) and using the average concentration in the capillary slit in eqn. (2) yields eqn. (7).

$$K_{\text{dim}} c_{\text{gen}} = \frac{c_{\text{D}}}{c_{\text{B}}^2} (c_{\text{B}} + 2c_{\text{D}}) = \left(\frac{c_{\text{D}}}{c_{\text{B}}}\right)^2 + \left(\frac{c_{\text{D}}}{c_{\text{B}}}\right) \quad (7)$$

By replacing the concentrations and equilibrium constant by eqn. (8):

$$K_{\text{dim}}(T) = \exp\left(\frac{\Delta_R G^\circ(T)}{RT}\right) = \exp\left(\frac{\Delta_R H^\circ - \Delta_R S^\circ T}{RT}\right) \quad (8)$$

eqn. (7) can be transformed into eqn. (9).

$$\ln\left[\left(\frac{A_{\text{ratio}}(T)}{\varepsilon_{\text{ratio}}}\right)^2 + \frac{A_{\text{ratio}}(T)}{\varepsilon_{\text{ratio}}}\right] - \ln[c_{\text{gen}}(T)] = -\frac{\Delta_R H^\circ}{RT} + \frac{\Delta_R S^\circ}{R} \quad (9)$$

with

$$A_{\text{ratio}} = \frac{A_{\text{D}}(T)}{A_{\text{B}}(T)}, \quad \varepsilon_{\text{ratio}} = \frac{\varepsilon_{\text{D}}}{\varepsilon_{\text{B}}}$$

and

$$c_{\text{gen}}(T) = c_{\text{init}} \left( \frac{A_{\text{A,init}}(T) - A_{\text{A}}(T)}{A_{\text{A,init}}(T_{\text{max}})} - \frac{A_{\text{P}}(T)}{A_{\text{P,sw}}} \right)$$

Equation (9) allows the determination of the standard reaction enthalpy and entropy as well as the ratio of the absorbance coefficients  $\varepsilon_{\text{D}}/\varepsilon_{\text{B}}$  by a non-linear fit of  $A_{\text{ratio}}(T)$  versus the temperature and the generated amount of radical and dimer  $c_{\text{gen}}(T)$ .

**Acknowledgements.** This project was financially supported in part by the Cooperation program PROCOPE 98 No. 98015 between the French *Ministère des Affaires Etrangères* and the German *Deutscher Akademischer Austauschdienst*.

## References

1. For a recent general review of conducting polymers and related oligomers, see for example: *Handbook of Organic Conductive Molecules and Polymers*; Nalwa, H. S. Ed., Wiley, New York, 1997.

- Garnier, F. *Angew. Chem., Int. Ed. Engl.* 28 (1989) 513.
- Roncali, J. *Chem. Rev.* 92 (1992) 711.
- For example see: Heeger, A. J. and Smith, P. In: Bredas, J. L. and Silbey, R., Eds., *Conjugated Polymers*, Academic Publishers, Dordrecht, The Netherlands 1991, pp. 141–210 and references cited therein.
- Hill, M. G., Mann, K. R., Miller, L. L., Penneau, J. F. and Zinger, B. *Chem. Mater.* 4 (1992) 1106.
- Hill, M. G., Mann, K. R., Miller, L. L. and Zinger, B. *Chem. Mater.* 4 (1992) 1113.
- Hill, M. G., Mann, K. R., Miller, L. L. and Penneau, J. F. *J. Am. Chem. Soc.* 114 (1992) 2728.
- Yu, Y., Gunic, E., Zinger, B. and Miller, L. L. *J. Am. Chem. Soc.* 118 (1996) 1013.
- Segelbacher, U., Sariciftci, N. S., Grupp, A., Bäuerle, P. and Mehring, M. *Synth. Met.* 57 (1993) 4728.
- Bäuerle, P., Segelbacher, U., Maier, A. and Mehring, M. *J. Am. Chem. Soc.* 115 (1993) 10217.
- Zotti, G., Schiavon, G., Berlin, A. and Pagani, G. *Chem. Mater.* 5 (1993) 430.
- Zotti, G., Schiavon, G., Berlin, A. and Pagani, G. *Chem. Mater.* 5 (1993) 620.
- Zuppiroli, L., Bussac, M. N., Paschen, S., Chauvet, O. and Forro, L. *Phys. Rev. B.* 50 (1994) 5196.
- Graf, D. D., Duan, R. G., Campbell, J. P., Miller, L. L. and Mann, K. R. *J. Am. Chem. Soc.* 119 (1997) 5888.
- Smie, A. and Heinze, J. *Angew. Chem., Int. Ed. Engl.* 36 (1997) 363.
- Tschuncky, P., Heinze, J., Smie, A., Engelmänn, G. and Koßmehl, G. *J. Electroanal. Chem.* 433 (1997) 223.
- Audebert, P., Guyard, L., Nguyen Dinh An, M., Groenendaal, L. and Meijer, E. W. *Chem. Mater.* 9 (1997) 723.
- Audebert, P., Hapiot, P., Pernaut, J.-M. and Garcia, P. *J. Electroanal. Chem.* 361 (1993) 283.
- Audebert, P., Hapiot, P., Monnier, K., Pernaut, J.-M. and Garcia, P. *Chem. Mater.* 6 (1994) 1549.
- Bard, A. J. and Faulkner, L. R. *Electrochemical Methods*, Wiley, New York 1980.
- Neudeck, A. and Dunsch, L. *J. Electroanal. Chem.* 370 (1994) 17.
- Neudeck, A. and Dunsch, L. *J. Electroanal. Chem.* 386 (1995) 138.
- Neudeck, A. and Dunsch, L. *Electrochim. Acta* 40 (1995) 1427.
- Garreau, D. and Savéant, J.-M. *J. Electroanal. Chem.* 35 (1972) 309.
- Crank, J. *Mathematics of Diffusion*, Clarendon Press, Oxford 1964.
- Simulations were made using an explicit finite method with a modification of a previously published procedure used for equilibrated reactions. See for example Andrieux, C. P., Hapiot, P. and Savéant, J.-M. *J. Electroanal. Chem.* 186 (1985) 237.

Received December 7, 1998.